



Corrosion Inhibition of α -Brass in 1 M Nitric Acid Solution by Medicinal Plants Extracts (Safflower)

A.S. Fouda^{1,*}, G.Y.El-Awady¹, A.Y. Elkateeb² and Aliaa M. Abd El-Haleem²

¹Chemistry Department, Faculty of Science, Mansoura University, Mansoura-35516, Egypt.

²Department of Agriculture Chemistry, Faculty of Agriculture, Mansoura University, Egypt.

ARTICLE INFO

Article history:

Received: 17 May 2015;

Received in revised form:

20 June 2015;

Accepted: 2 July 2015;

Keywords

Corrosion inhibition,
 α -brass, HNO₃,
Safflower plant extract.

ABSTRACT

The effect of the addition of safflower extract on the corrosion of α -brass in nitric acid done by chemical method (WL), electrochemical method "electrochemical impedance spectroscopy (EIS), potentiodynamic polarization, and electrochemical frequency modulation (EFM) technique". The efficiency of inhibition rise with increment the concentration inhibitor, but diminishes with expanding the temperature. The adsorption of safflower on the α -metal surface takes as Temkin adsorption isotherm. Impact of the temperature on the consumption of metal in one molar nitric corrosive was additionally mulled over. Potentiodynamic polarization studies demonstrated that safflower concentrates is blended sort inhibitor and the outcomes got from the systems are in great understanding.

© 2015 Elixir All rights reserved.

Introduction

Copper and its alloys, because of their excellent resistance to corrosion in neutral aggressive media and their ease of processing, they are widely used in industries, particularly as condensers and heat exchangers in power plants (1). Electrochemical techniques are effective tools to study brass since they offer profitable information about the phase and chemical composition (2). Such techniques have additionally proved to be useful to study the advancement of brass in the nature (3) to comprehend the degeneration process and to anticipate oxidation of the alloy better (4-5). Most of reported have as of late showed up in the literature (6-8) on the theme of inhibiting the corrosion of α -brass in acidic medium using green inhibitors, because they are non toxic and do not contain heavy metals hence they are environmentally friendly (9-10).

The aim of this paper is to describe corrosion of commercial 60/40 α -brass in 1 M HNO₃ solutions by safflower extract using weight-loss, potentiodynamic polarization measurements, electrochemical impedance spectroscopy (EIS) and electrochemical frequency modulation (EFM) measurements.

Experimental technique

Materials

The experiments were performed with local commercial α -brass (Helwan Company of Non-Ferrous Industries, Egypt) with the following composition (weight %) Cu63Zn37

Preparation of plant extracts

Safflower was used for coloring and flavoring food and making red and yellow dyes.

The dried safflower flowers sample. (100 g) of safflower mixed with 500ml boiling distilled water with stirring for 15min .then the aqueous extract was filtrated over cheese cloth and Whitman No. 1 paper respectively. The filtrates were frozen at -84°C in ultra -low temperature freezer.

Chemical result have shown that the safflower concentrate contain quino chalcones, flavonoids, alkaloids and polyacetylene (11).

Botanical aspect of safflower

Kingdom:	Plantae
(unranked):	Angiosperms
(unranked):	Eudicots
(unranked):	Asteraids
Order:	Asterales
Family:	Asteraceae
Genus:	Carthamus
Species:	C.tinctorius



Solutions

The corrosive solutions, 1 Molar HNO₃ were all set by dilution of analytical grade (67.5%) HNO₃ with bi-distilled water. All chemicals and reagents were of analytical grade. The measurements were performed in 1 M HNO₃ without and with the presence of the safflower extract in the concentration range (25ppm to 150ppm).

Bacterial agriculture media

Cut 50 g of the media in 1 L of distilled water and heat it to dissolve. Disinfect in oven at (121°C for 15 min), then Cool to 45-50°C, mix well and put into dishes. Leave the dishe to be

solid. The medium prepared should be at 8-15°C. The violet-red colour is appears.

Mass reduction (WL) method

The metal sheets were 2 × 2 × 2 cm with emery paper (grade 400–600–1200–2500) and then washed with bi-distilled water and acetone. After precise weighing, the metal sheet were put in a 100 ml beaker, which 100 ml of HNO₃ contained and without addition of various concentrations of safflower. All the aggressive acid solutions were open to air. After 3 h, the metal sheet were taken out, washed, dried, and weighed accurately. The average weight loss of the seven parallel α-brass sheets could be obtained. The inhibition efficiency (IE %) and the degree of surface coverage θ, of investigated compounds for the corrosion of α-brass in HNO₃ were calculated from Eq. (1) (12) :

$$IE \% = \theta \times 100 = [1 - (W / W^{\circ})] \times 100 \quad (1)$$

Where W^o and W are the values of the average weight loss without and with addition of the inhibitor, respectively

Electrochemical measurements

Tafel polarization methods

Polarization experiments were done in a classical three-electrode cell with a saturated calomel electrode (SCE) coupled to a fine Luggin capillary as reference electrode, platinum gauze as the auxiliary electrode and. The working electrode was cut in to 1×1cm from α-brass sheet of equal structure. Before each estimation, the surface of electrode was before experiment in the same method. Before measurements, the electrode was put in solution for half hour. every experiments were done in fresh prepared solutions at room temperature, then i_{corr} was used to calculate the inhibition efficiency and surface coverage (θ) as below:

$$\%IE = \theta \times 100 = [1 - (i_{corr} / i_{corr}^{\circ})] \times 100 \quad (2)$$

Where i_{corr}^o and i_{corr} are corrosion current densities in the absence and presence of inhibitor, respectively.

EIS methods

Result from Impedance were done using AC signals of 5 mV at the open circuit "the range of frequency from 100 kHz to 0.1 Hz". All result from technique were fitted to suitable to equivalent circuit using the Echem Gamry Analyst system version 6.03.

EFM technique

Data from EFM were done with applying perturbation potential signal with " amplitude 10 mV with two sine waves of 2 and 5 Hz". The frequencies sort from 2 and 5 Hz (13-14). The corrosion current density (i_{corr}) calculated by the larger peaks, the causality factors CF-2 and CF-3 and Tafel slopes (β_c and β_a) (15). Put the electrode potential in the solution to stabilize for half hour before the measurements start. All the experiments were done using Instrument Gamry Potentiostat/ Galvanostat/ ZRA (PCI4-G750) at room temperature. This contain a Gamry framework system v 6.03 Gamry applications include DC 105 software for DC corrosion measurements, EIS 300 software for electrochemical impedance spectroscopy measurements and EFM 140 for electrochemical frequency modulation measurements along with a computer for collecting data. Echem analyst v 6.03 software was used for plotting, graphing, and fitting data.

Surface examination

The surface films were formed on the α-brass specimens by immersing them in inhibitor solutions for a period of 24 h. After the immersion period, the specimens were taken out, dried and the nature of the film formed on the surface of the metal specimen was analyzed by EDX and SEM techniques. Examination of α-Brass surface after 24 h exposure to the 1 M HNO₃ solution without and with inhibitor was carried out by

JOEL JSM-6510LV Scanning Electron Microscope. Rough elemental analyses for the exposed surface were conducted by EDX technique.

Results and Discussion

Chemical Method (WL measurements)

Weight-loss of α brass was determined, at different time interims, in the absence and presence of various concentrations of safflower extracts. The obtained time weight-loss curves are shown in Figure 1 for safflower. The concentration of inhibitor affected on inhibition efficiency of corrosion. The digrams obtained in the presence of inhibitor fall significantly below that of free acid. In all cases, when the inhibitor concentration increase, weight-loss decrease and the inhibition percentage increase. These data lead to the deduction that the safflower are totally efficient as inhibitor for α brass dissolution in nitric acid solution. Also, the surface coverage degree (θ) by the inhibitor, calculated from Eq. (1), would increase by increasing the inhibitor concentration. The difference in the inhibition percentage (%IE) of inhibitor with their concentrations was calculated according to Eq. (1). The values obtained are reported in Table 1

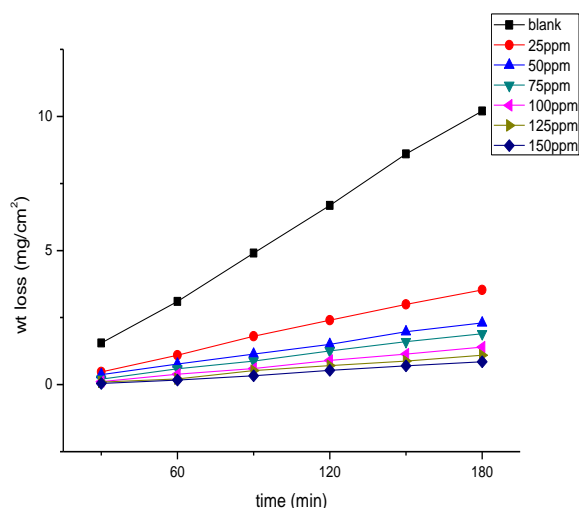


Figure 1. Weight loss-time curves for the corrosion of α brass in 1 M HNO₃ in the absence and presence of different concentrations of safflower inhibitor at 25°C

Effect of Temperature

The temperature effect on the corrosion rate of α brass in 1M HNO₃ and in presence of different concentrations of extract showed in the temperature range of 298–318K using weight loss measurements. As the temperature increases, the rate of corrosion increase and the inhibition efficiency of the additives decreases as shown in Table 2 for safflower. The adsorption behavior of extract on α brass surface is physical adsorption.

Adsorption Isotherm

The most advantage method for expressing adsorption quantitatively is by deriving the adsorption isotherm that describes the metal/inhibitor/ environment system. Different adsorption isotherms were applied to fit θ values, but the best fit was found to obey Temkin adsorption isotherm which are represented in Figure 2 for safflower, Temkin adsorption isotherm may be expressed by:

$$a \Theta = \ln K_{ads} C \quad (3)$$

Where C is the concentration (g/L) of the inhibitor in the bulk electrolyte, Θ is the degree of surface coverage (θ = % IE/100), K_{ads} is the adsorption equilibrium constant, and 'a' is heterogeneity factor. A plot of θ versus log C should give straight lines with the intercept equal log K_{ads}. The variation of

the adsorption equilibrium constant (K_{ads}) of the safflower with concentrations was measured according to Eq. (4). The data give good diagram fitting for obeyed isotherm adsorption as the coefficients correlation (R^2) were in the mean (0.943- 0.999). The values obtained are given in Table 3.

The equilibrium constant of adsorption K_{ads} obtained from the intercept of Temkin adsorption isotherm is related to the free energy of adsorption ΔG°_{ads} as follows:

$$K_{ads} = 1/55.5 \exp [-\Delta G^{\circ}_{ads} / RT] \tag{4}$$

Where 55.5 is the molar concentration of water in the solution in M^{-1} , R is the gas constant ($8.314 J mol^{-1} K^{-1}$), T the absolute temperature

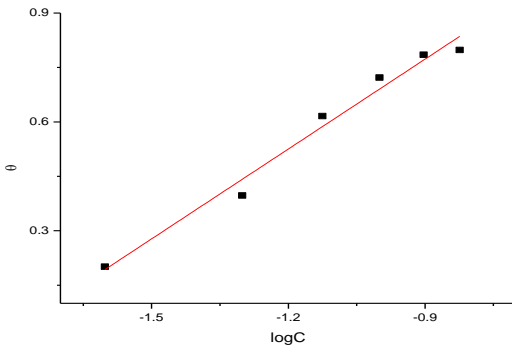


Figure 2: Temkin adsorption isotherm of safflower on α brass surface in 1 M HNO_3 at $25^{\circ}C$

The heat of adsorption (ΔH°_{ads}) and the standard entropy (ΔS°_{ads}) give according to the thermodynamic basic equation 5:

$$\Delta G^{\circ}_{ads} = \Delta H^{\circ}_{ads} - T \Delta S^{\circ}_{ads} \tag{5}$$

Table 3 shows ΔG°_{ads} good dependence on T, lead to the good relationship among thermodynamic parameters. The $-ve$ data of ΔG°_{ads} give the spontaneity adsorption process and stability layer adsorbed on surface of metal. Generally, data of ΔG°_{ads} average to $-20 kJ mol^{-1}$ or less are consistent with the interaction electrostatic between the charged metal and the charged molecules (physical adsorption); those average $-40 kJ mol^{-1}$ or larger contain charge transfer or sharing from organic molecules to the surface of metal to form a coordinate type (chemisorption) (16). The ΔG°_{ads} values are closer to $-20 kJ mol^{-1}$ lead to the mechanism of adsorption on metal in acidic medium was kind of physical adsorption (17). The parameter of thermodynamic result for the adsorption inhibitor Table 3 can rise valuable information about the corrosion inhibition mechanism. On other case the adsorption endothermic ($\Delta H^{\circ}_{ads} > 0$) is distributed unequivocally to chemisorption (18), an adsorption exothermic ($\Delta H^{\circ}_{ads} < 0$) may contain either chemisorption or physisorption mixture of both method. The calculated data of ΔH°_{ads} for the inhibitor adsorption acidic medium indicating inhibitor adsorbed physically. The ΔS°_{ads} of plant extract in 1M acidic medium are $-ve$. This mean that large in disorder obtain from reactants to the adsorbed metal- reaction (19).

Kinetic –thermodynamic corrosion parameter

The activation parameters for the corrosion process were calculated from Arrhenius-type plot according to eq. (6):

$$k_{corr} = A \exp (E_a^*/RT) \tag{6}$$

where E_a^* is the apparent activation corrosion energy, R is the universal gas constant, T is the absolute temperature and A is the Arrhenius pre-exponential constant. Values of apparent activation energy of corrosion for α brass in 1 M HNO_3 shown in Table 4, in the presence and absence of various concentrations of safflower obtain from the slope of $\log (k_{corr})$ against $1/T$ plots are draw in Figure 3. Indicating data draws that the energy

activation is larger in the presence of inhibitor. This lead to slow rate of adsorption of inhibitor with a resultant closer approach to equilibrium during the experiments at higher temperatures according to Hoar and Holliday (20). But, Hurd and Riggs (21) discuss minimize in the activation energy of corrosion at larger state of inhibition increasing from the net corrosion from metal surface. Huang and Schmid (22) obtain organic molecules inhibit both the cathodic and anodic partial reactions on the surface of electrode and a parallel reaction takes place on the area covered, but the rate of reaction on the covered area is substantially decrease than on the uncovered area similar to the present work.

The alternative formulation of transition state equation is shown in Eq. (7):

$$k_{corr} = (RT / Nh) e^{(\Delta S^*/R)} e^{(-\Delta H^*/RT)} \tag{7}$$

k_{corr} = the rate of metal dissolution, h = constant Planck’s, ΔH^* = the enthalpy of activation, ΔS^* = the entropy of activation and N = Avogadro’s number,. Figure 3 shows draw of $\log k$ against $(1/T)$ in safflower in 1 M HNO_3 . Straight lines are obtained with a slopes equal to $(\Delta H^*/2.303R)$ and intercepts are $[\log (R/Nh + \Delta S^*/2.303R)]$ are calculated Table 4. The increase in E_a^* with increase inhibitor concentration Table 4 is typical of physical adsorption. The positive signs of the enthalpies (ΔH^*) reflect the endothermic nature of the brass dissolution process. Entropies value (ΔS^*) mean that at the rate determining step the activated complex represents an association rather than a dissociation step, meaning that a decrease in disordering takes place on going from reactants to the activated complex (23-24). Although, the values (ΔS^*) gradually decrease with higher inhibitor concentration in all acid solution.

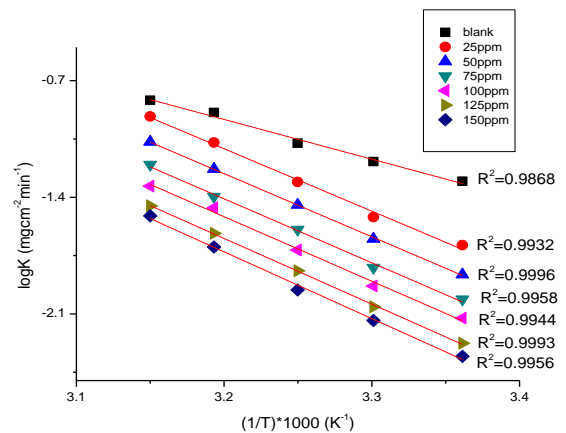


Figure 3: Arrhenius plots $\log k$ vs. $(1/T)$ curves for α brass corrosion rates (k_{corr}) at 120 minute of in 1M HNO_3 in with and without different concentrations of safflower

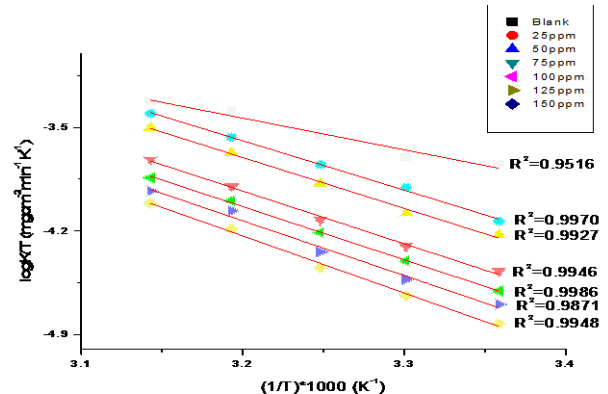


Figure 4. Transition plots $\log (k/T)$ vs. $(1/T)$ curves for α brass corrosion rates (k_{corr}) after 120 minute of immersion in

1M HNO₃ in the absence and presence of various concentrations of safflower.

Potentiodynamic Polarization Measurements

Figures 5 show typical polarization curves for α -brass in 1 M HNO₃ media. The two distinct regions that appeared were the active dissolution region (apparent Tafel), and the current limiting region. In the inhibitor-free the anodic diagram of copper illustrated a monotonic higher current with potential until the current the maximum value reached. the current density decrease with potential increase, lead to an anodic current peak which obeyed to formation Cu (NO₃)₂ film, both the anodic current and cathodic densities were greatly decreased over a wide potential range with inhibitor. Various corrosion parameters such as corrosion potential (E_{corr}), anodic and cathodic Tafel slopes (β_a , β_c), the corrosion current density (i_{corr}), the degree of surface coverage (θ) and the inhibition efficiency (%IE) are given in Tables 5.

It can see from the experimental results that in all cases, addition of inhibitors induced a significant decrease in cathode and anodic currents. The values of E_{corr} were affected and slightly changed by the addition of inhibitors. This indicates that these inhibitors act as mixed-type inhibitors. The slopes of anodic and cathodic Tafel lines (β_a and β_c), were slightly changed (Tafel lines are parallel), on increasing the concentration of the tested compounds which indicates that there is no change of the mechanism of inhibition in the presence and absence of inhibitors. The orders of inhibition efficiency of all inhibitor at different concentrations as given by polarization measurements are listed in Table 5.

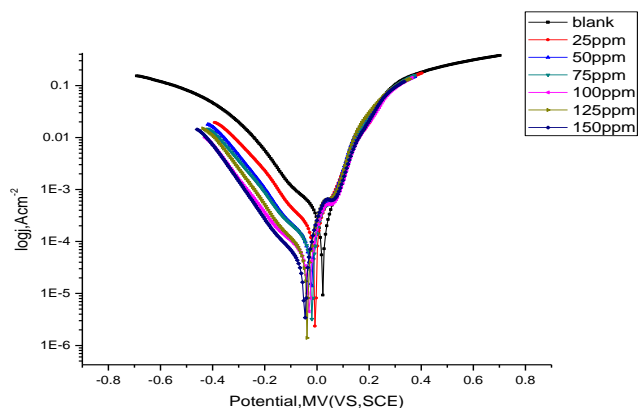


Figure 5: Potentiodynamic diagram for the dissolution of α brass in 1M HNO₃ with and without concentrations of safflower at 25°C

EIS method

EIS technique studying Surface properties, the corrosion, electrode kinetics and mechanistic obtained from diagrams impedance (25-29).

Figure 7 draw the Nyquist (a) and Bode (b) curves at room temperature. The higher size of the capacitive loop with safflower give the gradually barrier forms on metal surface. The capacitive loop is large in the size (Figure 7a) Bode curves (Figure 7b), give the total impedance increment with rise concentration of safflower (log Z against log f). But (log f against phase), and Bode diagram give the continuous large shift in the phase angle, otherwise relation with increase of adsorbed inhibitor on surface of metal. The Nyquist curves not give perfect semicircles as obtain from the EIS theory. The ideal semicircle shift was generally attributed to the dispersion frequency (30) in addition to the surface inhomogeneities.

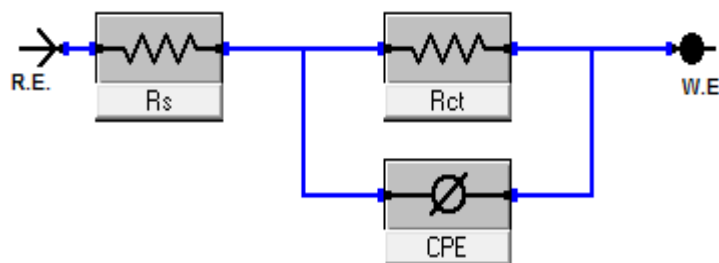


Figure 6: Circuit equivalent model utilized to fit method EIS safflower EIS spectra were analyzed utilized the equivalent circuit, Figure 6, given a reaction single charge transfer and our experimental results fits well. CPE, is capacitor of double layer give a more accurate fit (31). C_{dl} , a circuit contain a CPE parameter (Y_0 and n) were measure from eq.5 (32) :

$$C_{dl} = Y_0(\omega_{\max})^{-n-1} \quad (5)$$

Where Y_0 is the magnitude of the CPE, $\omega_{\max} = 2\pi f_{\max}$, f_{\max} is the frequency at which the impedance of imaginary component is maximal and n is the factor of parameter adjustable that usually lies between 0.50 and 1.0. then the diagram of the Nyquist plots analyzing, it is illustrate the diagrams approximated by a single capacitive semicircles, given the corrosion was mainly controlled charged-transfer (33,34). The general diagram of the curves is same behavior for all indicating that no change in the mechanism of corrosion (35). From the impedance result Table 6, we discussed that the value of R_{ct} increases with raising the inhibitor concentration and % IE_{EIS} increase, which in agreement with the data obtained from EFM. Actually the presence of inhibitor increase the value of R_{ct} in acidic solution. Values of double layer capacitance are also let down to the maximum range in the presence of extract and the decrease in the values of CPE obeys the order similar to that obtained for i_{corr} in this experiment. The CPE/ C_{dl} data decrease from a decrease in local dielectric constant and/or an increase in the thickness of the double layer, recommending that organic derivatives inhibit the corrosion of metal by adsorption at metal/acid (36, 37). Calculated the inhibition efficiency from the charge transfer resistance result from eq.8 (38):

$$\% \text{IE}_{\text{EIS}} = [1 - (R_{ct}^0 / R_{ct})] \times 100 \quad (8)$$

where R_{ct}^0 and R_{ct} are the charge-transfer resistance values without and with inhibitor respectively

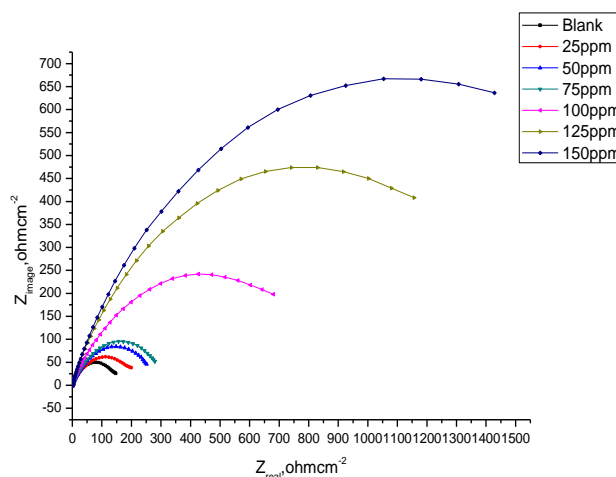


Figure 7a: The Nyquist plots for the corrosion of α brass in 1M HNO₃ in the absence and presence of different concentrations of safflower at 25°C

Table 1: Values of inhibition efficiencies (%IE) and surface coverage (θ) of safflower for the corrosion of α brass in 1 M HNO_3 from WL method at various concentrations and at 25°C

[inh], ppm	θ	% IE
25	0.641	64.1
50	0.775	77.5
75	0.811	81.1
100	0.865	86.5
125	0.894	89.4
150	0.921	92.1

Table 2: Values of inhibition efficiencies %IE and safflower corrosion rate (C.R) for the α brass corrosion in 1 M HNO_3 from WL method at various concentrations at temperature range of 298-318 K

[inh], ppm	298K		303K		308K		313K		318K	
	C.R	% IE	C.R	%IE	C.R	%IE	C.R	%IE	C.R	%IE
25	0.020	64.1	0.030	50.3	0.045	46.6	0.085	40.1	0.122	20.1
50	0.013	77.5	0.020	67.1	0.036	57.3	0.075	47.1	0.092	39.7
75	0.011	81.1	0.015	75.2	0.023	72.7	0.049	65.8	0.058	61.6
100	0.008	86.5	0.012	80.8	0.019	77.2	0.034	75.7	0.042	72.2
125	0.006	89.4	0.009	85.6	0.014	83.3	0.027	81.1	0.033	78.1
150	0.004	92.1	0.007	88.1	0.011	87.1	0.021	84.9	0.031	79.8

Table 3: Thermodynamic parameters for the adsorption of safflower on α brass surface in 1 M HNO_3 at different temperatures

Inhibitor	Temperature °C	K_{ads} M^{-1}	$-\Delta G^{\circ}_{\text{ads}}$ kJ mol^{-1}	$-\Delta H^{\circ}_{\text{ads}}$ kJ mol^{-1}	$-\Delta S^{\circ}_{\text{ads}}$ $\text{J mol}^{-1} \text{K}^{-1}$
safflower	25	2.811	29.6	134.9	0.353
	30	0.451	25.5		0.361
	35	0.272	24.6		0.358
	40	0.150	23.5		0.356
	45	0.068	21.8		0.356

Table 4: Activation of α brass corrosion in the presence and absence of brass corrosion in the absence and presence of various concentrations of safflower in 1M HNO_3

Inhibitor	[inh] ppm	E_a^* kJ mol^{-1}	ΔH^* kJ mol^{-1}	$-\Delta S^*$ J mol^{-1}	$A \times 10^7$ $\text{g cm}^{-2} \text{min}^{-1}$
Blank	0	45.9	18.3	134.03	6.70
safflower	25	58.5	27.9	60.9	10.84
	50	65.1	28.7	56.8	10.86
	75	65.8	29.8	53.4	10.87
	100	68.2	30.1	53.3	10.87
	125	69.4	30.9	48.9	10.97
	150	78.2	32.2	41.4	11.08

Table 5: Corrosion potential (E_{corr}), (β_c , β_a), (θ), (i_{corr}), and (% IE) of α brass in 1M HNO_3 at 25°C for safflower

Inhibitor	[inh] ppm	E_{corr} mV vs SCE	i_{corr} $\mu\text{A cm}^{-2}$	β_c mV dec^{-1}	β_a mV dec^{-1}	θ	% IE
Blank	0	22.3	389	200.9	110	----	----
safflower	25	-5.15	106	212.3	86.1	0.728	72.8
	50	-2.07	101	209.2	86.1	0.740	74.0
	75	-7.23	84.7	200.4	80.8	0.782	78.2
	100	-43.8	32.1	174	76.4	0.917	91.7
	125	-61.1	24	166.8	85.9	0.938	93.8
	150	-69.6	19.6	159.6	86.1	0.950	95.0

Table 6: Electrochemical kinetic parameters obtained by EIS technique for in 1 M HNO_3 without and with various concentrations of safflower at 25°C

Inhibitor	[inh] ppm	R_{ct} Ωcm^2	R_s Ωcm^2	C_{dl} μFcm^{-2}	θ	% IE
Blank	0	153.3	1.22	190	-----	-----
safflower	25	201.6	1.248	174	0.240	24.0
	50	268.5	1.586	172	0.429	42.9
	75	291.7	1.270	168	0.475	47.5
	100	715.0	1.547	166	0.786	78.6
	125	1282	1.607	130	0.880	88.0
	150	1773	1.597	128	0.914	91.4

Table 7: Electrochemical kinetic parameters obtained from EFM technique for α -brass in 1M HNO₃ in the absence and presence of different concentrations of safflower

Inhibitor	[inh] ppm	i_{corr} μAcm^{-2}	β_a mVdec^{-1}	β_c mVdec^{-1}	CF-2	CF-3	C.R mpy	θ	%IE
Blank	0	173.9	83	182	1.768	2.253	77.3	-	-
safflower	25	110.2	71	163	1.866	2.233	49.0	0.366	36.6
	50	84.1	68	151	1.904	2.272	37.4	0.516	51.6
	75	72.3	64	137	1.910	2.274	32.2	0.584	58.4
	100	31.7	79	140	1.890	2.210	14.1	0.818	81.8
	125	20.2	84	158	1.982	2.474	8.959	0.884	88.4
	150	15.2	83	144	2.191	3.071	6.768	0.912	91.2

Table 8: Surface composition (weight %) of α -brass before and after immersion in 1 M HNO₃ without and with 150 ppm of safflower at 25°C

(Mass %)	Cu	Zn	Fe	C	O	Al	As	Pt	Si
Free	60.78	32.72	0.79	3.48	1.13	0.70	0.40	----	----
blank	54.57	25.78	0.78	10.41	7.85	-----	0.61	-----	-----
safflower	56.53	16.33	----	18.32	7.01	-----	-----	1.63	0.19

Table 9. Data obtained from the plate counter for bacterial agriculture

Samples	CFU (R1)	CFU (R2)	CFU (mean)
Control	89 X 10 ⁴	95 X 10 ⁴	87 X 10 ⁴
Safflower	84 X 10 ⁴	90 X 10 ⁴	89 X 10 ⁴

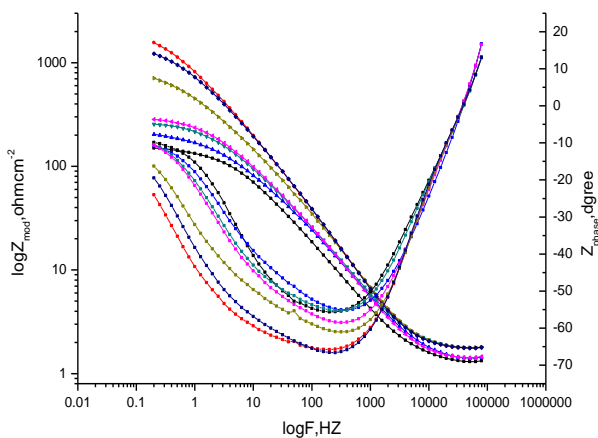


Figure 7b: The Bode plots for the corrosion of α brass in 1M HNO₃ in the absence and presence of different concentrations of safflower at 25°C

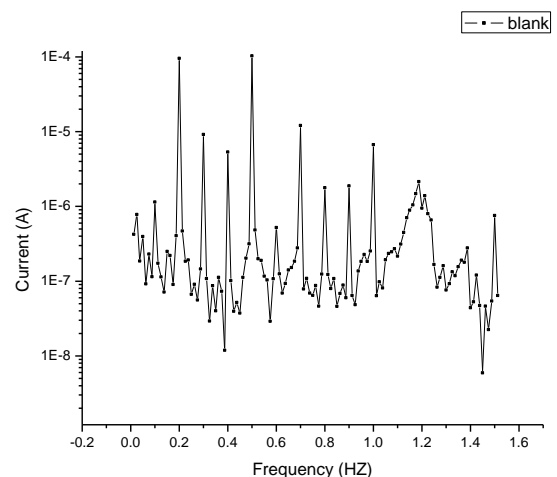
EFM method

Nondestructive technique for measuring corrosion that can quickly and directly determine the values of corrosion current without any information about Tafel slopes, and with only a short polarizing signal. These preferences of EFM technique make it an perfect candidate for online corrosion controlling (39). The causality factors is great strength of the EFM which do an inner check on the validity of estimation of EFM. The causality factors CF-2 and CF-3 are calculated from the frequency spectrum of the current responses. Figure 8 draw the EFM Intermodulation spectra (frequency vs current) of α -brass in HNO₃ solution containing safflower of various concentrations. The intermodulation and harmonic peaks are obviously visible and are much bigger than the background noise. The two large peaks, with amplitude of about 200 μA , are the reply to the 40 and 100 mHz (2 and 5 Hz) frequencies excitation. It is important to note that between the peaks there is nearly no current response (<100 nA). The EFM result were treated using two different models: complete diffusion control of

the cathodic reaction and the “activation” model. For the latter, a set of three non-linear equations had been solved, assuming that the corrosion potential does not change as result of the polarization of the working electrode (40). The corrosion current density (i_{corr}) calculated the larger peaks, the causality factors (CF-2 and CF-3) and the Tafel slopes (β_c and β_a). These parameters were recorded in Table 7. The presented data in Table 7 clearly show that, adding of any one of plant extract at a given concentration to the acidic solution the corrosion current density decreases, indicating that the plant extract inhibit the corrosion of α brass in 1 M HNO₃ through adsorption. The causality factors obtained under different experimental conditions are nearly equal to the theoretical values (2 and 3) that indicate the data measured are differ and of well quality. Increase the inhibition efficiencies %IE_{EFM} by increasing the inhibitor concentrations and was calculated as from Eq. (7):

$$\%IE_{EFM} = [1 - (i_{corr}/i_{corr}^0)] \times 100 \tag{7}$$

where i_{corr}^0 and i_{corr} are corrosion current densities in the absence and presence of inhibitor.



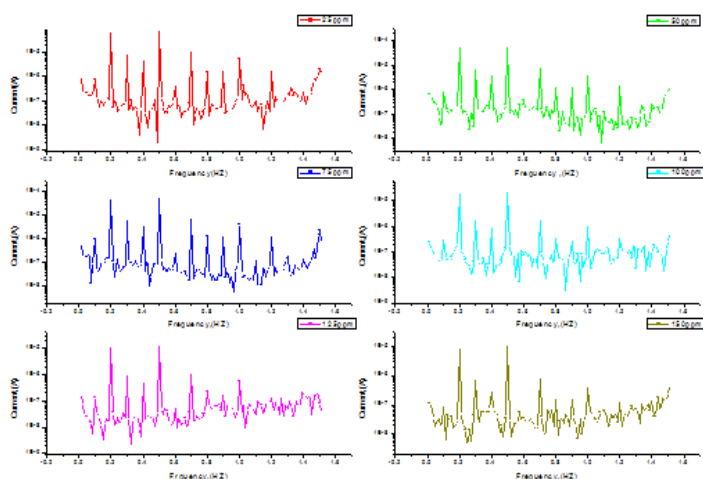


Figure 8: EFM spectra for α brass in 1 M HNO_3 in the absence and presence of different concentrations of safflower at 25 °C

SEM/EDX examination

In order to verify if the investigated compounds molecules are in fact adsorbed on α -brass surface, experiments of SEM and EDX were performed. The SEM micrographs for α -brass surface alone and after 24 h immersion in 1 M HNO_3 without and with the addition of 150ppm of the safflower is shown in Figures (9a-c). The corresponding EDX profile analyses are presented in Figures (10a-c). As expected, Figure 9a shows metallic surface is clear, while in the absence of the investigated plant extract, the α -brass surface is damaged by HNO_3 corrosion (Figure 9b). In contrast, in presence of the safflower (Figure 9c), the metallic surface seems to be almost no affected by corrosion. The corresponding EDX data are presented in Figures (10a-c) and Table 10. It is clear from the EDX spectra of α -brass in the presence of safflower, the appearance of C and O peaks (Figure 10c) which suggest the safflower adsorption on the α -brass surface and corroborate the thin inhibitor film formed and observed in SEM micrograph, thus protecting the surface against corrosion.

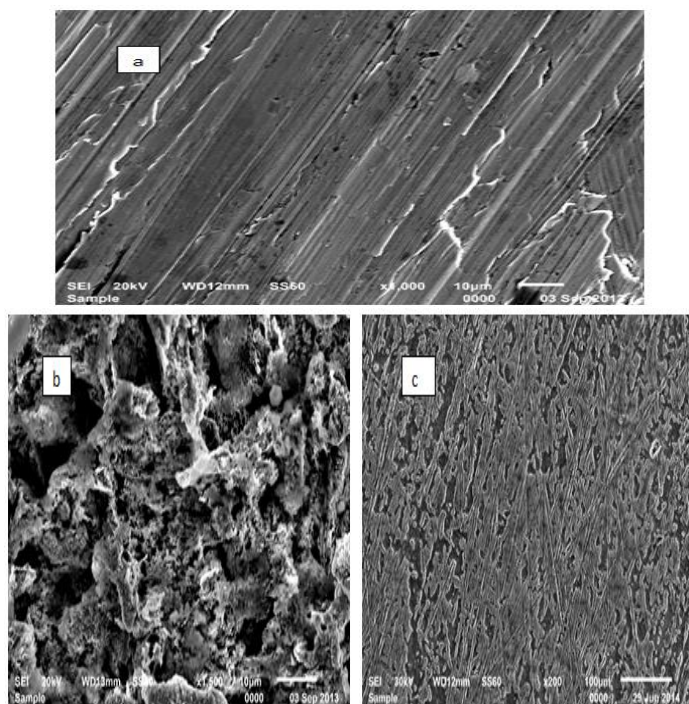


Figure 9: SEM micrographs of α -brass surface (a) before of immersion in 1 M HNO_3 , (b) after 24 h of immersion in 1 M HNO_3 , (c) after 24 h of immersion in 1 M HNO_3 +150ppm of safflower

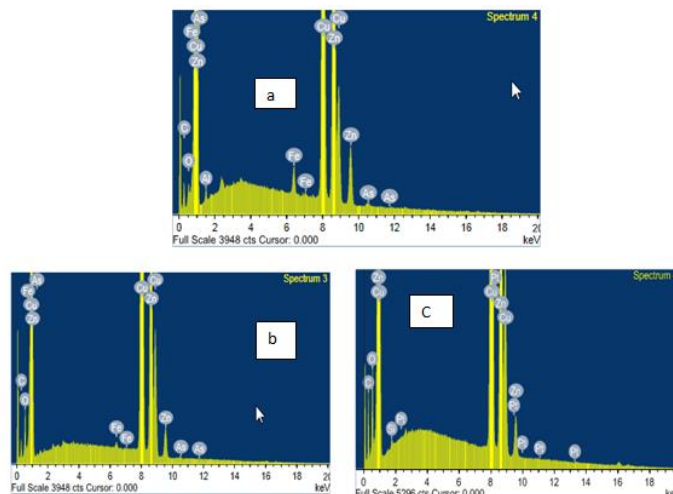
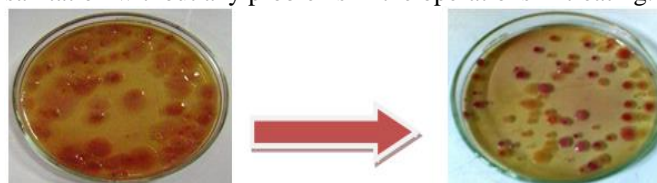


Figure 10: EDX spectra of of α -brass surface (a) before of immersion in 1 M HNO_3 , (b) after 24 h of immersion in 1 M HNO_3 , (c) after 24 h of immersion in 1 M HNO_3 + 150 ppm safflower extract.

Escherichia Coli Biological Effect

Agriculture Escherichia Coli bacteria with or without presence of Safflower inhibitor, Activity is small and Escherichia Coli colonies increase according to Table 11 and Fig.11. Inhibitor has oxygen, and nitrogen donor atom linked with the proteins and lipids on the bacterial tissues existence activity for it respiration by oxygen atom release and nutrition by nitrogen atom. So this extract has no poisoning on the activity of bacterial, and can be used safety on the plants sanitation without any problems in the operations in treating.



Blank *the bacterial agriculture in 150 ppm safflower*

Figure 11. The bacterial agriculture with and without Safflower inhibitor

Mechanism of Corrosion inhibition

Inhibition efficiency of aqueous extract safflower is due to its phytochemical constituents. Most of these phytochemicals are organic compounds that have center for π electron. The major constituents of safflower are flavonoids, alkaloids, poly acetylene and quino chalcone. Inhibition efficiency of aqueous extracts of safflower is due to formation of multi-molecular layer of adsorption between copper in α -brass and some of these photochemical.

4. Conclusions

The results from the study the following may be concluded:

- I. safflower extract is good corrosion inhibitor for α -brass in 1 M HNO_3 solution.
- II. Reasonably good agreement was observed between the data obtained from the weight loss and electrochemical measurements were in good agreement.
- III. Results obtained from potentiodynamic polarization is mixed-type inhibitor.
- IV. Percentage inhibition efficiency of safflower is temperature dependent and its addition led to a decrease of the activation corrosion energy in all the studied acid media.
- V. The thermodynamic parameters revealed that the inhibition of corrosion by safflower is due to the formation of a physical adsorbed film on the metal surface.

VI. The adsorption of safflower onto α - brass surface follows the Temkin adsorption isotherm model.

VII. Thus safflower extract was proved to be an effective eco-friendly and low cost inhibitor.

VIII. This inhibitor has no effect on the biological activity of *Escherichia Coli*, and can be applying safety on sanitation plants.

References

- Li, S.L., Ma, H.Y., Lei, S.B., Yu, R., Chen, S.H., and Liu, D.X., "Inhibition of Copper Corrosion with Schiff Base Derived from 3-Methoxysalicylaldehyde and O-Phenyldiamine in Chloride Media. *Corrosion* 54, (1998) 947-954.
- Stevanovic J., Skibina L. J., Stefanovic M., Despic A., Jovic V. D., "Phase structure analysis of brass by anodic linear –sweep voltammetry", *J. Appl Electrochem.* 22, (1992) 172-178.
- Habib K., Amin A. "Electrochemical behaviour of α -brass in natural sea water", *Desalination* 85, (1992) 275-28.
- Morales J., Fernandez G. T., Esparza P., Gonzalez S., Sa R. C. "A comparative study on the passivation and localized corrosion of α , β , and $\alpha+\beta$ brass in borate buffer solutions", *Corros. Sci.* 37, (1995) 211-229.
- Badawy W. A., Al-Kharafi F. M. "Oxide plasticity in the oxidation mechanism of zirconium and its alloys", *Corros. Sci.* 5, (1999) 268-268.
- Samar.Y.Al_nami, "Effect of 4-phenyl 4-phenylthiazole derivatives on preventing dezincification of α -brass in acid chloride solution", *J. Mater. Environ. Sci.*, 4(1)(2013)39-48.
- Mihit M., El Issami S., Bouklah M., Bazzi L., Hammouti B., Ait Addi E., Salghi R. and Kertit S. "the inhibited effect of some tetrazolic compounds towards the corrosion of brass in nitric acid solution", *Appl Surf Sci.* 252 (6), (2006) 2389-2395.
- Alkharafi F.M., Ghayad I.M., Abdullah R.M. "Effect of hydrogen peroxide on the dezincification of brass in acidified sodium sulfate solution under free corrosion condition". *J. Mater. Environ. Sci.* 1 (1)(2010) 58-69.
- M. Aquraishi N. Kumar, B.N. Singh, SK Singh., "Calcium palmitate: Agreeen corrosion inhibitor for steel in concrete environment.", *J. Mater. Environ. Sci.* 3(6)(2012)1001-1008.
- O. Benali, H. Benmehdi, O. Hasnaoui, C. selles, R. Salghi, "Green corrosion inhibitor :inhibitive action of tanin extract of chamaerops humillis plant for the corrosion of mild steel in 0.5M H₂SO₄". *J. Mater. Environ. Sci.* 4(1)(2013)117-126.
- shijunyue, yupingtang, chengneixu, slinjioliandjin-aoduan "two new quinochalcone C-Glycosides from the florets of *carthamus tinctorius*" *Molecular Science* 15, (2014), 16760-16771.
- Mu, G.N., Zhao, T.P., Liu, M., Gu, T, "Effect of metallic cations on corrosion inhibition of an anionic surfactant for mild steel". *Corrosion* 52 (1996) 853-856.
- Khaled K. F., "Evaluation of electrochemical frequency modulation as a new technique for monitoring corrosion and corrosion inhibition of carbon steel in perchloric acid using hydrazine carbodithioic acid derivatives", *J. Appl. Electrochem.*, 39 (2009) 429-438
- Bosch R. W., Hubrecht J., Bogaerts W. F., Syrett B. C., "Electrochemical frequency modulation: A new electrochemical technique for online corrosion monitoring". *Corrosion* 57 (2001) 60-70.
- Abdel-Rehim S. S., Khaled K. F., Abd-Elshafi N. S., *Electrochim. Acta* 51 (2006) 3269.
- Yurt A, Bereket G, Kivrak A, Balaban A & Erk B, "Effect of Schiff bases containing pyridyl group as corrosion inhibitors for low carbon steel in 0.1M HCl", *J Appl Electrochem*, 35 (2005) 1025-1032.
- Bentiss F, Traisnel M & Lagrenee M, " The substituted 1,3,4-oxadiazole :A new class of corrosion inhibitors of mild steel in acidic media", *Corros. Sci.*, 42 (2000) 127-146.
- Durnie W, Marco R D, Jefferson A & Kinsella B, "Development of structure activating relationship for oil field corrosion inhibitor", *J Electrochem Soc*, 146 (1999) 1751-1756.
- Banerjee G & Malhotra S N, "contribution to adsorption of aromatic amines on mild steel surface from HCL solutions by impedance, Uv and Raman spectroscopy". *Corrosion*, 48 (1992) 10-15.
- Hour T P & Holliday R D, "The inhibition by quino lines and thioureas of the acid dissolution of mild steel", *J Appl Chem*, 3 (1953) 502-513.
- Riggs L O (Jr) & Hurd T J, "Temperature coefficient of corrosion inhibition", *Corrosion*, 23 (1967) 252-288.
- Schmid G M & Huang H J, "spectro-electro chemical studies of the inhibition effect of 4,7 -di phenyl -1,10 phenoanthroline on the corrosion of 304 stainless steel, *Corros. Sci.*, 20 (1980) 1041-1057.
- Bentiss F, Lebrini M & Lagrenee M, "Thermodynamic characterization of metal dissolution and inhibitor adsorption processes in mild steel /2,5-bis (n-thienyl)-1,3,4-thiadiazoles, hydrochloric acid system *Corros. Sci.*, 47 (2005) 2915-2931.
- Marsh J, *Advanced Organic Chemistry*, 3rd edn (Wiley Eastern, New Delhi), 1988.
- Silverman D.C. and Carrico J. E., "Electrochemical impedance technique- A practical tool for corrosion prediction", *Corrosion*, 44(1988) 280-287.
- Lorenz W. J. and Mansfeld F., "Determination of corrosion rates by electrochemical DC and AC methods", *Corros. Sci.* 21 (1981) 647-672.
- Macdonald D. D., Mckubre M. C., "Impedance measurements in Electrochemical systems," *Modern Aspects of Electrochemistry*, J.O'M. Bockris, B.E. Conway, R.E. White, Eds., Vol. 14, Plenum Press, New York, New York, P 61, 1982.
- Mansfeld F. "Recording and analysis of AC impedance Data for corrosion studies". *Corrosion*, 36(1981) 301-307.
- Gabrielli C., "Identification of Electrochemical processes by Frequency Response Analysis," *Solarton Instrumentation Group*, 1980.
- El Achouri M., Kertit S., Gouttaya H.M., Nciri B., Bensouda Y., Perez L., Infante M.R., Elkacemi K., Prog. corrosion inhibition of iron in 1M HCl by some gemini surfactants in the series of alkanediyl- α - ω -bis(dimethyl tetra decyl ammonium) ", *Org. Coat.*, 43 (2001) 267-273.
- Macdonald J.R., Johanson W.B., in: J.R. Macdonald (Ed.), *Theory in Impedance Spectroscopy*, John Wiley & Sons, New York, 1987.
- Mertens S. F., Xhoffer C., Decooman B. C., E. Temmerman, "Short-Term deterioration of polymer-coated 55% Al-Zn- part Li behavior of thin polymer films", *Corrosion*, 53 (1997) 381-388.
- Trabanelli G., Montecelli C., Grassi V., Frignani A., "Electrochemical study on inhibitors of rebar corrosion in carbonated concrete", *J. Cem. Concr., Res.*, 35 (2005) 1804-1813.
- Trowsdate A. J., Noble B., Haris S. J., Gibbins I.S. R., Thomson G. E., Wood G. C., "The influence of silicon carbide reinforcement on the pitting behaviour of aluminum " *Corros. Sci.*, 38 (1996) 177-191.
- Reis F. M., De Melo H.G. and Costa I., "Impedance spectroscopy: over 35 years electrochemical sensor optimization", *Electrochim. Acta*, 51 (2006) 6217-6229.
- Lagrenee M., Mernari B., Bouanis M., Traisnel M. & Bentiss F., "study of the mechanism and inhibiting efficiency of

3,5-bis(4-methy thiophenyl)-4H-1,2,4triazole on mild steel corrosion in acidic media", *Corros. Sci.*, 44 (2002) 573-588.

37. McCafferty E., Hackerman N., "Double layer capacitance of iron and corrosion inhibition with poly methylene diamines", *J. Electrochem. Soc.*, 119 (1972) 146-154.

38. Ma H., Chen S., Niu L., Zhao S., Li S., Li D., J. "inhibition of copper corrosion by several Schiff bases in aerated halide solutions", *Appl. Electrochem.*, 32 (2002) 65-72.

39. Kus E., Mansfeld F., "An evaluation of the electro chemical frequency modulation (EFM) technique", *Corros. Sci.* 48 (2006) 965-979.

40. Caigman G. A., Metcalf S. K., Holt E. M., "Thio phene substituted dihydro pyridines *J.Chem. Cryst.*, 30 (2000) 415-422.